HHS Public Access

Author manuscript

Cell Rep. Author manuscript; available in PMC 2024 July 18.

Published in final edited form as:

Cell Rep. 2024 June 25; 43(6): 114335. doi:10.1016/j.celrep.2024.114335.

The interaction between RIPK1 and FADD controls perinatal lethality and inflammation

Diego A. Rodriguez[1,8], **Bart Tummers**[2,8,*], **Jeremy J.P. Shaw**[1], **Giovanni Quarato**[1,3], **Ricardo Weinlich**[4], **James Cripps**[5], **Patrick Fitzgerald**[1], **Laura J. Janke**[6], **Stephane Pelletier**[7], **Jeremy Chase Crawford**[1,9], **Douglas R. Green**[1,10,*]

[1]Department of Immunology, St. Jude Children's Research Hospital, 262 Danny Thomas Place, Memphis, TN 38105, USA

[2]Centre for Inflammation Biology & Cancer Immunology (CIBCI), Department of Inflammation Biology, School of Immunology & Microbial Sciences, King's College London, London SE1 1UL, UK

[3]Treeline Biosciences, San Diego, CA 92121, USA

[4]Hospital Israelita Albert Einstein, São Paulo, Brazil

[5]Center for Cancer Immunology and Immunotherapy, Brown Cancer Center, University of Louisville School of Medicine, Louisville, KY, USA

[6]Department of Pathology, St. Jude Children's Research Hospital, 262 Danny Thomas Place, Memphis, TN 38105, USA

[7]Department of Medical and Molecular Genetics, Indiana University Genome Editing Center, Indiana University School of Medicine, Indiana University, Indianapolis, IA 46902, USA

[8]These authors contributed equally

[9]Present address: Department of Host-Microbe Interactions, Center for Infectious Diseases Research, St. Jude Children's Research Hospital, 262 Danny Thomas Place, Memphis, TN, 38105, USA

[10]Lead contact

SUMMARY

*Correspondence: bart.tummers@kcl.ac.uk (B.T.), douglas.green@stjude.org (D.R.G.).

AUTHOR CONTRIBUTIONS

Conceptualization, D.A.R., B.T., J.J.P.S., G.Q., R.W., P.F., J.C.C., and D.R.G.; investigation, D.A.R., B.T., J.J.P.S., G.Q., R.W., and L.J.J.; formal analysis, D.A.R., B.T., J.J.P.S., G.Q., R.W., L.J.J., J.C.C., and D.R.G.; writing the paper, D.A.R., B.T., and D.R.G.; journal contact, B.T.; corresponding author, B.T. and D.R.G.; production of new reagents or analytic tools, J.C., P.F., and S.P.; supervision, D.R.G.; funding acquisition, D.R.G.; lead contact, D.R.G. First authorships are listed in alphabetical order.

DECLARATION OF INTERESTS

D.R.G. consulted for Sonata Pharmaceuticals, Ventus Pharmaceuticals, and ASHA Therapeutics and received grant support from Amgen during this research.

SUPPLEMENTAL INFORMATION

Supplemental information can be found online at https://doi.org/10.1016/j.celrep.2024.114335.

Perturbation of the apoptosis and necroptosis pathways critically influences embryogenesis. Receptor-associated protein kinase-1 (RIPK1) interacts with Fas-associated via death domain (FADD)-caspase-8-cellular Flice-like inhibitory protein long ($cFLIP_L$) to regulate both extrinsic apoptosis and necroptosis. Here, we describe *Ripk1*-mutant animals (*Ripk1*^{R588E} [RE]) in which the interaction between FADD and RIPK1 is disrupted, leading to embryonic lethality. This lethality is not prevented by further removal of the kinase activity of *Ripk1* (*Ripk1*$^{R588E\ K45A}$ [REKA]). Both *Ripk1*^{RE} and *Ripk1*^{REKA} animals survive to adulthood upon ablation of *Ripk3*. While embryonic lethality of *Ripk1*^{RE} mice is prevented by ablation of the necroptosis effector mixed lineage kinase-like (MLKL), animals succumb to inflammation after birth. In contrast, *Mlkl* ablation does not prevent the death of *Ripk1*^{REKA} embryos, but animals reach adulthood when both MLKL and caspase-8 are removed. Ablation of the nucleic acid sensor *Zbp1* largely prevents lethality in both *Ripk1*^{RE} and *Ripk1*^{REKA} embryos. Thus, the RIPK1-FADD interaction prevents Z-DNA binding protein-1 (ZBP1)-induced, RIPK3-caspase-8-mediated embryonic lethality, affected by the kinase activity of RIPK1.

In brief

Rodriguez et al. show that breaking the interaction between the cell-death-regulating proteins RIPK1 and FADD results in developmental death and inflammation that are initiated by the cellular receptor ZBP1 and regulated by the kinase activity of RIPK1, shedding light on the intricate functions of this interaction.

Graphical Abstract

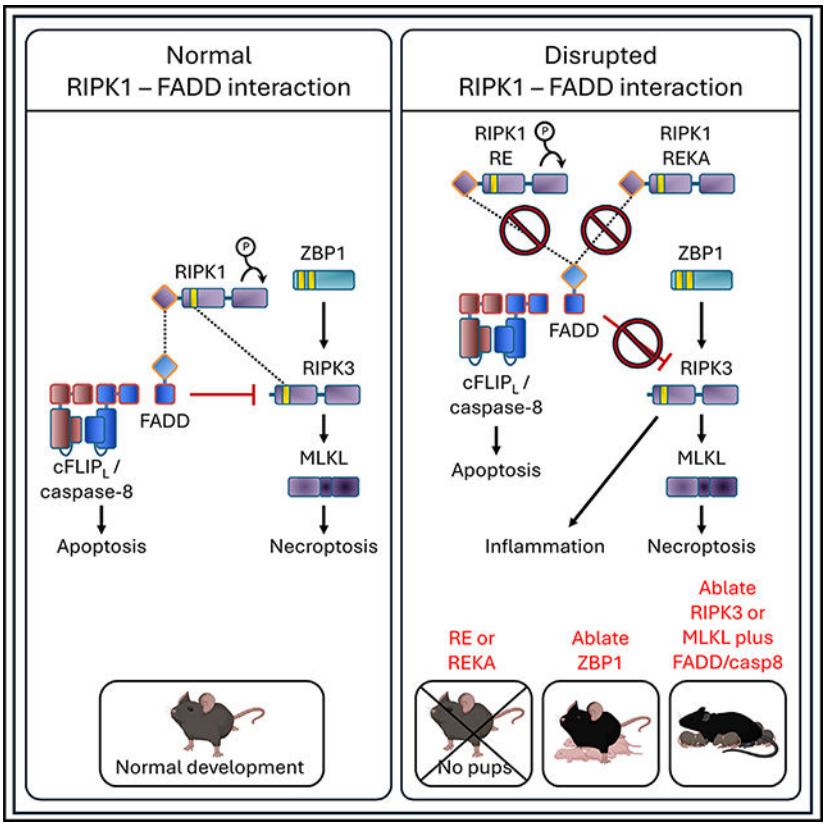

INTRODUCTION

Necroptosis is a regulated cell death that plays important roles in the control of infection, inflammation, and tissue damage.[1] Activation of the kinase receptor-associated protein kinase-3 (RIPK3) leads to phosphorylation and activation of mixed lineage kinase-like (MLKL), which then oligomerizes and destroys the integrity of cell membranes, including the plasma membrane, resulting in necrotic cell death. A RIP kinase homology interacting motif (RHIM) in RIPK3 oligomerizes with both RIPK3 and another kinase, RIPK1, and the latter binds to the protein Fas-associated via death domain (FADD) via DDs in both proteins. FADD then recruits Caspase-8, which oligomerizes and is thereby activated to cleave RIPK1 and RIPK3. Consequently, when RIPK3 is activated, the FADD-Caspase-8 complex prevents ensuing necroptosis. Inhibition or ablation of FADD or Caspase-8 thus promotes necroptosis, which is underscored by the findings that fully penetrant embryonic lethality observed in *Casp8*- or *Fadd*-deficient mice at embryonic day (E) 10.5 is completely prevented by ablation of either *Ripk3* or *Mlkl*.[2–4]

RIPK3 is activated by RHIM-RHIM interactions that are initiated by the RHIM domains of any of three proteins: RIPK1, TIR domain-containing adapter-inducing interferon (TRIF), and Z-DNA binding protein-1 (ZBP1).[5] Tumor necrosis factor receptor-1 (TNFR1) ligation activates RIPK1 to activate RIPK3.[6,7] Toll-like receptor (TLR)-3 and -4 ligation induces TRIF to activate RIPK3.[8] ZBP1 expression is induced by interferon signaling[9] and is

activated by Z-RNAs to activate RIPK3.[10] In each case, the presence of RIPK1 recruits the FADD-Caspase-8 complex, thereby preventing necroptosis.

In addition to activating MLKL, RIPK3 can also induce the activation of FADD-Caspase-8 to cause apoptosis.[8,11] Another protein, cellular Flice-like inhibitory protein long ($cFLIP_L$, herein FLIP), prevents Caspase-8 oligomerization and apoptosis but nevertheless activates Caspase-8 to cleave RIPK1 and prevent necroptosis. This is underscored by the observation that the embryonic lethality of FLIP-deficient mice is prevented by co-ablation of *Fadd* and either *Ripk3* or *Mlkl*.[2,12]

A further complication of this pathway was revealed when an inactive mutant of Caspase-8 resulted in embryonic lethality that was not prevented by the ablation of *Ripk3* or *Mlkl*.[13,14] These Caspase-8 mutant, RIPK3-deficient animals died at a later embryonic stage due to the activation of Caspase-1.[13,14] This appears to be due to an ability of inactive Caspase-8 to bind to poptosis-associated speck-like protein (ASC), which in turn binds and activates Caspase-1.[15]

RIPK1-deficient animals survive gestation but die around birth.[16] These animals survive to adulthood by co-ablation of either *Fadd* or *Casp8* and either *Ripk3* or *Mlkl*.[17,18] Thus, RIPK1 represents a “node” that connects the FADD-Caspase-8 and RIPK3-MLKL pathways. We therefore sought to determine the effects of disrupting the interaction between the DDs of RIPK1 and FADD, with or without a kinase-inactivating mutation in RIPK1. We generated animals with such mutations, and these resulted in embryonic lethality, consistent with our understanding of this system. However, crossing these animals to animals lacking RIPK3, MLKL, caspase-8, FADD, or ZBP1 revealed unexpected phenotypes that further inform the complexity of these interactions and provide insights into the role of RIPK1 in homeostasis.

RESULTS

Abrogating the interaction between FADD and RIPK1 is incompatible with embryonic survival

Human RIPK1 interacts with FADD via its arginine 603 residue (R603, R588 in mouse).[19] To investigate how this interaction regulates necroptosis, we utilized our murine model systems and mutated the positively charged R588 of RIPK1 to negatively charged glutamic acid (R588E). We then reconstituted *Ripk1*$^{-/-}$ mouse embryonic fibroblasts with doxycycline-inducible wild-type (WT), kinase-inactive (K45A), R588E-mutant, or R588E,K45A (REKA) double-mutant RIPK1. Stimulation with poly I:C, combined with the pan-caspase-inhibitor zVAD-fluoromethyl ketone (zVAD), induced the interaction between FADD and RIPK1 WT or K45A but not RIPK1 R588E or REKA (Figure 1A), indicating that the murine R588 residue mediates the interaction between mouse RIPK1 and FADD, similar to human R603.[19] RIPK1 R588E- and REKA-expressing cells underwent necroptosis upon treatment with poly I:C, whereas RIPK1 WT-expressing cells required the addition of zVAD. RIPK1 K45A-expressing cells did not undergo death under any of these conditions (Figures S1A and S1B).[20] Thus, the R588E mutation abrogates the interaction

between RIPK1 and FADD, preventing the recruitment of the FADD-Caspase-8-cFLIP$_L$ complex to block necroptosis.

The FADD-Caspase-8-cFLIP$_L$ complex inhibits TNF-induced necroptosis during embryogenesis, since *Fadd*$^{-/-}$,[21] *Casp8*$^{-/-}$,[22] or *Cflar*$^{-/-}$ (encoding cFLIP$_L$)[23] embryos do not develop past E10.5 unless one of the proteins that mediate necroptosis, i.e., RIPK3 or MLKL, is co-ablated.[2–4,12] Embryonic lethality at E10.5 in the necroptosis-proficient animals is protected until approximately E16.5 by ablation of TNFR1.[17] We therefore hypothesized that the RIPK1 R588E mutation should result in the induction of necroptosis in developing embryos at E10.5.

We generated RIPK1 R588E (*Ripk1*$^{RE/RE}$) and kinase-inactive (K45A) RIPK1 R588E (*Ripk1*$^{REKA/REKA}$) mutant animals and assessed their embryonic development. Although *Ripk1*$^{RE/RE}$ pups were not found at birth, embryos developed past the expected E10.5 and survived up to 16.5 days post-gestation (Figure 1B). Similarly, *Ripk1*$^{REKA/REKA}$ embryos were not found at birth but developed up to 19.5 days post-gestation (Figure 1C). These data suggest that the RIPK1 R588E mutation allows the inhibition of TNFR1-dependent necroptosis at E10.5 and reveals a time point during embryogenesis (~E16.5) where embryos receive signals that induce their demise, mediated by the kinase activity of RIPK1.

To examine why the RIPK1 R588E mutation inhibited TNFR1-induced necroptosis, we immunoprecipitated the TNFR1 complex from *Ripk1*$^{WT/WT}$ and *Ripk1*$^{RE/RE}$ murine embryonic fibroblasts (MEFs) and observed that the RIPK1 R588E mutation reduced the ability of RIPK1 to bind TNFR1 (Figure S2A). TNF stimulation induced RIPK1 cleavage in *Ripk1*$^{WT/WT}$, but not *Ripk1*$^{RE/RE}$, MEFs (Figure S2B). TNF and cycloheximide stimulation induced robust cell death in *Ripk1*$^{WT/WT}$ and *Ripk1*$^{REKA/REKA}$ MEFs (Figure S2C). TNF plus LCL-161, which induces RIPK1-dependent apoptosis,[24,25] induced death in *Ripk1*$^{WT/WT}$ MEFs, but not *Ripk1*$^{REKA/REKA}$ MEFs and did so more slowly in and *Ripk1*$^{RE/RE}$ MEFs (Figure S2D). Thus, the RIPK1 R588E mutation reduces binding to TNFR1 and delays TNF plus LCL-161-induced apoptosis. This is consistent with the idea that the RE mutation reduces association with the DDs of both TNFR1 and FADD.

Activation of TLR3 by poly I:C can lead to TRIF-RIPK3-MLKL-mediated necroptosis, which is blocked by the RIPK1-recruited FADD-Caspase-8-cFLIP$_L$ complex, where RIPK1 interacts with RIPK3 through RHIM interactions and FADD via DD interactions.[8,26,27] Similar to RIPK1 R588E-expressing MEFs (Figures S1A and S1B), primary *Ripk1*$^{RE/RE}$ and *Ripk1*$^{REKA/REKA}$ MEFs generated from our mutant mice died when exposed to poly I:C, unlike their WT counterparts (Figures 1D and 1E). Immunoprecipitation of endogenous RIPK1 from poly I:C plus zVAD-treated MEFs co-precipitated FADD from *Ripk1*^{WT}- or *Ripk1*^{K45A}-expressing MEFs but not from *Ripk1*^{RE}- or *Ripk1*^{REKA}-expressing MEFs (Figure S1C). Conversely, RIPK3 and MLKL co-precipitated with RIPK1^{RE} or RIPK1^{REKA} but much less so with RIPK1^{WT} or RIPK1^{K45A}.

Lethal RIPK3-dependent necroptosis and inflammation in the absence of the RIPK1-FADD interaction

Since the embryonic lethality of *Fadd*$^{-/-}$ or *Casp8*$^{-/-}$ mice can be prevented by co-ablating *Ripk3* or *Mlkl*[2–4,12] and the RIPK1 R588E mutation abrogates the block of necroptosis by the FADD-Caspase-8-cFLIP$_L$ complex, we hypothesized that ablation of these necroptotic genes may prevent the embryonic lethality of *Ripk1*$^{RE/RE}$ and *Ripk1*$^{REKA/REKA}$ mice. Ablating *Ripk3* from *Ripk1*$^{RE/RE}$ (Figure 2A) or *Ripk1*$^{REKA/REKA}$ mice (Figure 2B) yielded viable animals, indicating that the embryonic lethality of *Ripk1*$^{RE/RE}$ and *Ripk1*$^{REKA/REKA}$ animals is dependent on RIPK3. Both genotypes developed normally; however, *Ripk1*$^{REKA/REKA}$ *Ripk3*$^{-/-}$ mice died after several weeks of life (Figure 2C). In contrast, no mortality was observed in *Ripk1*$^{RE/RE}$ *Ripk3*$^{-/-}$ animals (Figure 2C).

To determine if the lethal effects of RIPK3 in our mutant mice were exclusively due to necroptosis, we ablated the necroptosis effector MLKL. *Ripk1*$^{RE/RE}$ *Mlkl*$^{-/-}$ mice were born at a sub-Mendelian frequency (Figure 3A); approximately 50% of these animals did not survive past weaning, and all died by ~60 days (Figures 3B and 3C). *Ripk1*$^{RE/RE}$ *Mlkl*$^{-/-}$ pups and weaned animals were significantly smaller than littermate *Ripk1*$^{WT/WT}$ *Mlkl*$^{-/-}$ and *Ripk1*$^{WT/RE}$ *Mlkl*$^{-/-}$ mice and showed evidence of anemia and lymphopenia (Figures S3A and S3B). Necropsy revealed that *Ripk1*$^{RE/RE}$ *Mlkl*$^{-/-}$ pups exhibited inflammation in colon and skin (Figures 3D and 3E) and other tissues, as well as hyperplasia in colon, bone marrow, and liver tissues, and hypocellularity of lymphoid organs (Figures S3C–S3G). Moreover, gene expression analysis of liver tissue by RNA sequencing revealed that several pathways associated with inflammatory and interferon responses were upregulated in *Ripk1*$^{RE/RE}$ *Mlkl*$^{-/-}$ pups as compared to the *Ripk1*$^{WT/RE}$ *Mlkl*$^{-/-}$ littermates (Figure 3F). These results suggest that RIPK3 mediates lethal inflammation, which is inhibited by the FADD-RIPK1 interaction.

It was plausible that the abrogated interaction between FADD and RIPK1 R588E would allow the FADD-Caspase-8-cFLIP$_L$ complex to induce inflammatory processes, which could lead to the pathology of the *Ripk1*$^{RE/RE}$ *Mlkl*$^{-/-}$ animals. We therefore ablated *Fadd* from *Ripk1*$^{RE/RE}$ *Mlkl*$^{-/-}$ mice. *Fadd*$^{-/-}$ *Ripk1*$^{RE/RE}$ *Mlkl*$^{-/-}$ mice were born (Figure 3G) and survived (Figure 3H) similarly to *Ripk1*$^{RE/RE}$ *Mlkl*$^{-/-}$ mice. *Fadd*$^{-/-}$ *Ripk1*$^{WT/RE}$ *Mlkl*$^{-/-}$ littermate mice succumbed to lyphoproliferative (LPR) disease, whereas *Fadd*$^{-/-}$ *Ripk1*$^{RE/RE}$ *Mlkl*$^{-/-}$ mice did not (Figures S3H–S3J). These data indicate that the FADD-Caspase-8-cFLIP$_L$ complex does not contribute to the RIPK3-mediated inflammation in *Ripk1*$^{RE/RE}$ *Mlkl*$^{-/-}$ mice.

Caspase-8 drives the death of developing *Ripk1*$^{REKA/REKA}$ *Mlkl*$^{-/-}$ embryos

Our data suggested that RIPK3 drives the lethality of developing *Ripk1*$^{REKA/REKA}$ embryos (Figure 2B). However, ablation of *Mlkl* did not prevent the embryonic death of *Ripk1*$^{REKA/REKA}$ embryos (Figure 4A), indicating that *Ripk1*$^{REKA/REKA}$ embryos do not die by engaging necroptosis. RIPK3 is known to mediate necroptosis or Caspase-8-mediated apoptosis when its ability to induce necroptosis is inhibited,[8,11,28] suggesting that *Ripk1*$^{REKA/REKA}$ *Mlkl*$^{-/-}$ embryos could succumb to Caspase-8-mediated apoptosis. We therefore ablated *Casp8* from *Ripk1*$^{REKA/REKA}$ *Mlkl*$^{-/-}$ mice and observed that this

prevented embryonic lethality (Figure 4B). Thus, RIPK3 is able to induce a Caspase-8-dependent lethal signal when RIPK1 is unable to interact with FADD. Our results with the *Ripk1*$^{RE/RE}$ *Mlkl*$^{-/-}$ mice (Figure 3A) suggest that this lethal effect is blocked by the kinase activity of RIPK1. *Casp8*$^{-/-}$ *Ripk1*$^{REKA/REKA}$ *Mlkl*$^{-/-}$ mice did not develop the inflammatory phenotype observed in the *Fadd*$^{-/-}$ *Ripk1*$^{RE/RE}$ *Mlkl*$^{-/-}$ animals but did succumb at a time similar to *Casp8*$^{-/-}$ *Ripk1*$^{WT/REKA}$ *Mlkl*$^{-/-}$ mice (Figure 4C), displaying lymphadenopathy and splenomegaly. We confirmed that this was LPR, as the peripheral blood contained large numbers of TCRβ+, B220+ cells[29] (Figure 4D).

ZBP1 drives the death of developing *Ripk1*$^{RE/RE}$ and *Ripk1*$^{REKA/REKA}$ embryos

Our genetic data indicated that RIPK3 drives death of developing *Ripk1*$^{RE/RE}$ and *Ripk1*$^{REKA/REKA}$ embryos. However, the mechanisms that activate RIPK3 in this setting remained unclear. RIPK3 can mediate cell death upon activation of TNFR1,[6,30,31] TRIF-activating TLRs (TLR3 and −4),[8] or ZBP1.[32] In developing embryos, TNFR1 is expressed at E10,[33] causing death of *Casp8*$^{-/-}$ embryos at E10.5.[17] Since both *Ripk1*$^{RE/RE}$ and *Ripk1*$^{REKA/REKA}$ embryos develop beyond the E10.5 time point, we reasoned that TNFR1-mediated RIPK3 activation is not involved in *Ripk1*$^{RE/RE}$ and *Ripk1*$^{REKA/REKA}$ embryonic lethality. ZBP1 is a cytosolic receptor that recognizes endogenous Z-nucleic acids,[34] although the identity of these endogenous sequences and when these sequences are expressed remains to be determined. ZBP1 is expressed in response to type I and II interferons,[9] and our previous work showed that FADD and Caspase-8 control the expression of ZBP1 under homeostatic conditions.[35] Moreover, we and others previously demonstrated that FADD-Caspase-8 and RIPK1 form a complex that regulates gene expression.[36–39] This led us to surmise that the interaction between RIPK1 and FADD-Caspase-8 controls the expression of ZBP1. We therefore assessed ZBP1 expression in our RIPK1-reconstituted MEF cells and observed that ZBP1 expression is upregulated in cells expressing RIPK1 R588E or REKA but not WT or K45A (Figure 5A). Moreover, ZBP1 expression was present in tissues of *Ripk1*$^{RE/RE}$ *Ripk3*$^{-/-}$ and *Ripk1*$^{REKA/REKA}$ *Ripk3*$^{-/-}$ mice (Figure 5B), indicating that the interaction between RIPK1 and FADD controls the expression of ZBP1.

These results suggested that ZBP1 may be responsible for the activation of RIPK3-mediated death during embryogenesis. Therefore, we ablated *Zbp1* from *Ripk1*$^{RE/RE}$ and *Ripk1*$^{REKA/REKA}$ animals. Viable *Ripk1*$^{RE/RE}$ *Zbp1*$^{-/-}$ and *Ripk1*$^{REKA/REKA}$ *Zbp1*$^{-/-}$ mice were born, albeit at non-Mendelian frequencies (Figures 5C and 5D), indicating that ZBP1 functions as an endogenous receptor that is engaged during embryonic development to induce RIPK3-mediated death.

Ripk1$^{RE/RE}$ *Zbp1*$^{-/-}$ pups succumbed pre-weaning (Figure 5E) with signs of mild inflammation, hyperplasia, and cell death in various tissues (Figures S4A and S4B). However, *Ripk1*$^{REKA/REKA}$ *Zbp1*$^{-/-}$ mice weaned and survived up to 165 days (Figure 5F), suggesting that the kinase activity of RIPK1 is also involved in the induction of inflammation in this setting.

DISCUSSION

Here, we have interrogated two murine lines, both containing an R588E mutation in RIPK1 (RIPK1^{RE}) that disrupts its interaction with FADD and one containing an additional K45A mutation in RIPK1^{RE} (RIPK1^{REKA}) that disrupts kinase activity. Since the interaction of RIPK1 with FADD is critical for Caspase-8 activation and cleavage-mediated disruption of RIPK1 activity,[40–42] and since the K45A mutation does not prevent embryonic lethality in *Fadd*$^{-/-}$ mice,[43] we predicted that both RIPK1 variants would be lethal. Consistent with this, homozygous animals of either allele resulted in embryonic lethality that was dependent on RIPK3, as is embryonic lethality caused by ablation of caspase-8 or FADD.[2–4,12] However, unlike *Casp8*$^{-/-}$ or *Fadd*$^{-/-}$ animals, which consistently die at E10.5, *Ripk1*$^{RE/RE}$ and *Ripk1*$^{REKA/REKA}$ animals die later in gestation. It is possible that the R588E mutation only partially prevents association with FADD, resulting in a delayed lethal effect. The lethality in these mice was partially prevented by ablation of ZBP1, allowing the birth of a fraction of the homozygous animals, an effect that has not been described for either *Casp8*$^{-/-}$ or *Fadd*$^{-/-}$ animals.

Unlike *Ripk1*$^{RE/RE}$ and *Ripk1*$^{REKA/REKA}$ mice, *Ripk1*$^{-/-}$ mice survive gestation. This suggests that RIPK1 has functions other than controlling cell death that may drive embryonic lethality. Indeed, the interaction between RIPK1 and FADD controls the expression of ZBP1, as the expression of RIPK1^{RE} or RIPK1^{REKA}, but not RIPK1^{WT}, in *Ripk1*$^{-/-}$ *Mlkl*$^{-/-}$ MEFs results in ZBP1 expression, and ZBP1 acts as a driver of embryonic death during gestation of our mutant animals. ZBP1 expression during embryogenesis may thus depend on RIPK1 and may be blocked by FADD-Caspase-8 and would therefore not occur in developing *Ripk1*$^{-/-}$ mice. Consistent with these observations, *Casp8*$^{-/-}$ *Mlkl*$^{-/-}$ and *Fadd*$^{-/-}$ *Mlkl*$^{-/-}$ mice express ZBP1 and active RIPK3 in several organs, and this is dependent on a cGAS-STING-interferon signaling pathway.[35] Therefore, it is possible that the same pathway is engaged in embryos in which RIPK1 does not interact with FADD, as in our mutant mice.

It remains unclear how ZBP1 is activated to induce RIPK3-mediated lethality as the precise cell intrinsic signals that activate ZBP1 have not been elucidated to date. Z-RNAs are a suggested ligand for ZBP1.[10] Endogenous retroviral elements, which are known to be transiently expressed in developing embryos around E15,[44] have also been postulated as potential activators of ZBP1.[45] However, we were previously unable to detect these in mice lacking Caspase-8 activity where ZBP1 was active.[35] The RIPK1-induced transcriptional profile may potentially generate endogenous Z-RNA species that are able to activate ZBP1, as is observed in animals lacking caspase-8 or FADD (and MLKL).[35] However, such endogenous Z-RNA forms have not yet been identified *in vivo*.

Although ZBP1 deficiency only partially prevents the death of *Ripk1*$^{RE/RE}$ and *Ripk1*$^{REKA/REKA}$ mice, it fully prevents the perinatal lethality of *Ripk1*$^{RHIM/RHIM}$ mice, in which the critical RHIM motif IQIG is mutated to AAAA.[46,47] In this setting, ZBP1 drives necroptosis, since death of *Ripk1*$^{RHIM/RHIM}$ mice is prevented by disruptions in the functioning of RIPK3, e.g., by catalytic inactivity (RIPK3 D161N), RHIM-mutant RIPK3 or RIPK3 deficiency, or MLKL deficiency.[46,47] This indicates that RIPK1 RHIM prevents

ZBP1 activation of RIPK3 and downstream necroptosis around the time of birth. Our observations indicate that the death of *Ripk1*$^{RE/RE}$ and *Ripk1*$^{REKA/REKA}$ mice is mediated by ZBP1 in conjunction with other pathways. TRIF signaling can activate RIPK3-mediated necroptosis, suggesting that TRIF may play a role in the lethality of *Ripk1*$^{RE/RE}$ and *Ripk1*$^{REKA/REKA}$ mice, although TRIF deficiency does not prevent the death of *Ripk1*$^{RHIM/RHIM}$ mice.[46,47] We have not, however, formally tested the idea that TRIF signaling contributes to lethality in our ZBP1-deficient RIPK1-mutant mice.

The roles of the RIPK1 DD in regulating the various functions of RIPK1 have been explored. A RIPK1 DD mutation, K599R (human)/K584R (mouse), was reported to disrupt RIPK1 DD homodimerization but not its kinase activity or its role in TNFR1-induced gene expression.[48] Although the K584R mutation effectively prevented RIPK1 association with FADD, TNF-induced phosphorylation of MLKL was blocked by this mutation. Consequentially, *Ripk1*$^{K584R/K584R}$ mice are viable.[48] The RIPK1 K584R mutation thus contrasts with the RIPK1 R588E mutation explored here, which allows necroptosis signaling.

The functions of the kinase activity of RIPK1 in regulating embryonic death are elusive. *Ripk1*$^{RE/RE}$ embryos (E16.5) die earlier than *Ripk1*$^{REKA/REKA}$ embryos (E19) but are born when *Mlkl*$^{-/-}$ is ablatsed, whereas *Ripk1*$^{REKA/REKA}$ *Mlkl*$^{-/-}$ mice do not survive gestation. Kinase-inactive RIPK1 prevents TNFR1-, TLR3/4-, and ZBP1-induced necroptosis,[7,8,20] but RIPK1 itself is only required for necroptosis induced by the ligation of TNFR1. This may explain why *Ripk1*$^{REKA/REKA}$ embryos appear to die later than *Ripk1*$^{RE/RE}$ embryos. Because the ablation of RIPK3 preserved survival to adulthood of both mutant mice, our results on the effects of MLKL ablation suggest that the kinase activity of RIPK1 prevents a lethal, necroptosis-independent function(s) of RIPK3 that is independent of MLKL. This RIPK3-mediated lethality manifests during gestation in *Ripk1*$^{REKA/REKA}$ *Mlkl*$^{-/-}$ mice. Another lethal function of RIPK3 may be responsible for death post-parturition in *Ripk1*$^{RE/RE}$ *Mlkl*$^{-/-}$ animals.

The death of *Ripk1*$^{RE/RE}$ embryos is mediated by RIPK3 and MLKL and thus necroptosis. The death of *Ripk1*$^{REKA/REKA}$ embryos, however, depends on RIPK3 but not MLKL. In the case of *Ripk1*$^{REKA/REKA}$ *Mlkl*$^{-/-}$ mice, the necroptosis-independent, lethal function of RIPK3 is driven by Caspase-8, since *Casp8*$^{-/-}$ *Ripk1*$^{REKA/REKA}$ *Mlkl*$^{-/-}$ mice survive gestation and reach adulthood. One study has shown that RIPK3 engages caspase-8 in the absence of the RIPK1-FADD interaction in a direct fashion, as interferon-induced ZBP1- and RIPK3-dependent Caspase-8 activation was observed in *Ripk1*$^{-/-}$ cells.[9] Another possibility is that RIPK3 indirectly causes Caspase-8-dependent lethality. TRADD can complex with FADD to drive Caspase-8 activation in 18.5-day-old *Ripk1*$^{-/-}$ embryos.[49] How *Ripk1*$^{RE/RE}$ and *Ripk1*$^{REKA/REKA}$ mutants might regulate this remains unclear.

Ripk1$^{RE/RE}$ *Mlkl*$^{-/-}$ mice develop an inflammatory pathology that is not observed in *Ripk1*$^{RE/RE}$ *Ripk3*$^{-/-}$ animals, implying that RIPK3 drives MLKL-independent inflammation when the FADD-RIPK1 interaction is disrupted. We postulated that RIPK3 may engage FADD-Caspase-8 to mediate inflammation, but this is not the case, since *Fadd*$^{-/-}$ *Ripk1*$^{RE/RE}$ *Mlkl*$^{-/-}$ mice show a similar inflammatory pathology. In contrast,

Casp8$^{-/-}$ *Ripk1*$^{REKA/REKA}$ *Mlkl*$^{-/-}$ mice do not display the inflammatory phenotype seen in *Fadd*$^{-/-}$ *Ripk1*$^{RE/RE}$ *Mlkl*$^{-/-}$ animals, although they eventually succumb to LPR disease, as expected.[2] It remains to be determined if Caspase-8 plays a FADD-independent role in driving the inflammatory pathology of *Ripk1*$^{RE/RE}$ *Mlkl*$^{-/-}$ mice, possibly through interaction with ASC and caspase-1.[38,39]

Unexpectedly, *Fadd*$^{-/-}$ *Ripk1*$^{RE/RE}$ *Mlkl*$^{-/-}$ mice did not develop LPR disease but apparently succumbed to the inflammatory pathology observed in *Fadd*$^{+/+}$ *Ripk1*$^{RE/RE}$ *Mlkl*$^{-/-}$ mice with similar kinetics. This is surprising, since in every other scenario where *Fadd*-deficient mice are viable, *Fadd* deficiency confers the development of LPR disease, e.g., in *Fadd*$^{-/-}$ *Ripk3*$^{-/-}$, *Fadd*$^{-/-}$ *Mlkl*$^{-/-}$, *or Fadd*$^{-/-}$ *Casp8*$^{DA/DA}$ *Casp1/11*$^{-/-}$ *Mlkl*$^{-/-}$ mice.[2,39] It is unclear why the inflammatory phenotype, driven by the RIPK1 RE mutation, takes precedent over the development of LPR disease, but these results suggest that ongoing inflammation may suppress the LPR phenotype. Since *Casp8*$^{-/-}$ *Ripk1*$^{REKA/REKA}$ *Mlkl*$^{-/-}$ mice develop LPR, the data further suggest that the RIPK1 kinase activity may be responsible for driving inflammation and suppressing LPR disease. Although FADD blocks caspase-8-driven inflammasome activation in epithelial cells,[38,39] the similar kinetics of survival in *Fadd*$^{+/+}$ and *Fadd*$^{-/-}$ *Ripk1*$^{RE/RE}$ *Mlkl*$^{-/-}$ mice suggest that this effect is not responsible for the inhibition of LPR. Since LPR disease is believed to be a result of abrogated Fas-induced apoptosis, elucidating how LPR may be prevented in *Fadd*$^{-/-}$ *Ripk1*$^{RE/RE}$ *Mlkl*$^{-/-}$ mice may enhance our understanding of LPR disease.

Limitations of the study

This study has not investigated possible roles of TRIF or TRADD in preventing the embryonic lethality of *Ripk1*$^{RE/RE}$ or *Ripk1*$^{REKA/REKA}$ mice. Possible roles for Caspase-8 in driving the inflammatory phenotype of *Ripk1*$^{RE/RE}$ *Mlkl*$^{-/-}$ animals have not been assessed.

STAR★METHODS

RESOURCE AVAILABILITY

Lead contact—Further information and requests for resources and reagents should be directed to the lead contact, Douglas R. Green (douglas.green@stjude.org).

Materials availability—Experimental models generated in this study are available upon reasonable request.

Data and code availability

- RNA sequencing data have been deposited into the Short Reach Archive (SRA) under BioProject: PRJNA983782.
- This paper does not report original code.
- Any additional information required to reanalyze the data reported in this paper is available from the lead contact upon request.

EXPERIMENTAL MODEL AND STUDY PARTICIPANT DETAILS

Animals—All mice were bred and housed (5 maximum) in pathogen-free facilities, in a 12-h light/dark cycle in ventilated cages, with chow and water supply *ad libitum*. The St. Jude Institutional Animal Care and Use Committee approved all procedures in accordance with the Guide for the Care and Use of Animals. *Ripk3*$^{-/-}$,[50] *Mlkl*$^{-/-}$,[51] *Casp8*$^{-/-}$ *Mlkl*$^{-/-}$[17] and *Fadd*$^{-/-}$ *Mlkl*$^{-/-}$,[2] mice have been previously described. *Ripk1*$^{RE/RE}$ mice were generated by insertion of the point mutation of RIPK1 at the Arg (R) to Glu (E) in the position 588 (R588E, RE) was engineered by using CRISPR/Cas9 technology. The sgRNAs and Cas9 mRNA transcripts were designed and generated as described previously.[52] The target site for each sgRNA is unique in the mouse genome, and no potential off-target site with fewer than two mismatches was found using the Cas-OFFinder algorithm.[53] Briefly, St. Jude Transgenic/Gene Knockout Shared Resource injected pronuclear-staged C57BL/6J zygotes with a single-guide RNA (Key Resource Table; 125 ng/μL) introducing a DNA double-stranded break into the *Ripk1* gene in the chromosome 13, human codon-optimized Cas9 mRNA transcripts (50 ng/μL), and a single-stranded DNA molecule containing the desired change on the aminoacidic change Ripk1-R588E-HDR (Key Resource Table). To facilitate the identification of founder mice and genotyping, silent substitutions generating a HindIII restriction site (5′-AAGCTT-3′) were also introduced. Zygotes were surgically transplanted into the oviducts of pseudopregnant CD1 females, and newborn mice carrying the Ripk1-R588E allele were identified by PCR (821 bp), HindIII-restriction digestion (387 + 434 bp), and Sanger sequencing by using specific designed primers, respectively (Key Resource Table). The generation of a single mutation of RIPK1 at the Lys (K) to Ala (A) in the position 45. Single-guide RNA (Key Resource Table) (125 ng/μL) and a single-stranded DNA molecule containing the desired change on the aminoacidic change Ripk1-K45A-HDR were used. (Key Resource Table). The identification of founder mice and genotyping, silent substitutions generating a AgeI restriction site (5′-GTCTACACCGGT-3′) were also introduced. Newborn mice carrying the Ripk1-K45A allele were identified by PCR (680 bp), AgeI-restriction digestion (244 + 437 bp), and Sanger sequencing by using specific designed primers, respectively (Key Resource Table). Accordingly, *Ripk1*$^{REKA/REKA}$ mice was generated by mutation of at the Lys (K) to Ala (A) in the position 45 and Arg (R) to Glu (E) in the position 588 (K45A-R588E, REKA) with a double injection of the single-guide RNAs plus the Ripk1-R588E-HDR and Ripk1-K45A-HDR, respectively. Identification of newborn mice carrying the Ripk1-RE or Ripk1-REKA was performed by using the respective PCR primers as indicated above. Mouse age ranged from gestation to >200 days and both male and female mice were used. For all studies, mice were age- and sex-matched.

Cultured cell lines—Primary murine embryonic fibroblasts (MEF) of the indicated genotypes were generated as recently described ([35]). Briefly, ~E12–14.5 embryos were homogenized generating a single cell suspension plated in complete DMEM media containing 10% FBS, L-glutamine, pen/strep, 55 mM β-mercaptoethanol, 1 mM sodium pyruvate and non-essential amino acids (GIBCO). All experiments on primary *Ripk1*$^{RE/RE}$ or *Ripk1*$^{REKA/REKA}$ MEF were performed on cells at passage 2–4. Immortalization of *Ripk1*$^{-/-}$ primary MEF were performed by infection with SV40 large T antigen and maintained in complete DMEM media as indicated.

METHOD DETAILS

Reconstitution of *Ripk1*$^{-/-}$ or *Ripk1*$^{-/-}$ *Mlkl*$^{-/-}$ MEFs—The mouse *Ripk1* WT, or K45A, R588E or R588E K45A mutant constructs were cloned in frame with a T2A-GFP sequence into the pBABE-puro retroviral expression vector or alternatively into Dox-inducible vector pRetroX-TRE3G (Clontech). Retroviruses were produced using Phoenix-AMPHO cells co-expressing psPAX2 and pVSVg plasmids (Addgene) and our pBABE-puro or pRetroX-TRE3G vectors using Lipofectamine 2000 (Thermo Fisher Scientific). Retrovirus containing supernatants were har-vested and filtered 48 h post-transfection. *Ripk1*$^{-/-}$ iMEFs transduced to stably express DOX-inducible RIPK1 constructs were selected with puromycin (2 mg/mL) or for the pBABE constructs selected three times by FACS sort based on GFP+.

Cell death quantification—Cell death kinetic was quantified in real-time by using an Incucyte S3 Live Cell Imaging and Analysis (Sartorius). Briefly, plated cells were incubated in complete DMEM media containing the specified treatments plus 0.5 mg/mL Propidium Iodide (PI). At the endpoint, all cells were permeabilized (100% PI^{+}) by addition of 25 mg/mL of Digitonin (D141, Sigma). Dead cells were quantified by using Incucyte image analysis software (Sartorius). Data was expressed as percentages of the ratio PI^{+}/Digitonin (PI^{+} %).

Immunoprecipitation and Immunoblot—Immunoprecipitations were performed using the Dynabeads Co-Immunoprecipitation Kit (Invitrogen) following manufacturer instructions. Briefly, pelleted cells were lysed in lysis buffer supplemented with proteases (Roche) phosphatases (Roche) inhibitors. Primary antibodies against anti-FADD (Santa Cruz Biotechnologies) or anti-RIPK1 (Cell Signaling) were covalently coupled to Dynabeads M-270 Epoxy beads or anti-FLAG M2 Affinity Gel (Sigma). Immunoprecipitations were performed following manufacturer recommendations (Invitrogen). Elution products were diluted in 4x XT sample buffer (Bio-Rad) and boiled at 95 C for 5 min. After SDS-PAGE resolution (Bio-Rad), proteins were transferred onto nitrocellulose (Bio-Rad). Membranes were blocked with 3% BSA in PBS 1.0% Tween and incubated with the indicated antibodies (Key Resource Table). Bound antibodies were visualized using ChemiDoc Touch Imaging System (Bio-Rad).

RNA sequencing—Total RNA was isolated from liver tissue of *Ripk1*$^{WT/REKA}$ *Mlkl*$^{-/-}$ and *Ripk1*$^{REKA/REKA}$ *Mlkl*$^{-/-}$ mice. Briefly, RNA purification was performed using the RNeasy Kit (QIAGEN) according to manufacturer instructions. RNA was quantified using the Quant-iT RiboGreen RNA assay (ThermoFisher) and quality checked by the 2100 Bioanalyzer RNA 6000 Nano assay (Agilent) or 4200 TapeStation High Sensitivity RNA ScreenTape assay (Agilent) prior to library generation. Libraries were prepared from total RNA with the TruSeq Stranded Total RNA Library Prep Kit according to the manufacturer's instructions (Illumina, PN 20020599). Libraries were analyzed for insert size distribution using the 2100 BioAnalyzer High Sensitivity kit (Agilent), 4200 TapeStation D1000 ScreenTape assay (Agilent), or 5300 Fragment Analyzer NGS fragment kit (Agilent). Libraries were quantified using the Quant-iT PicoGreen dsDNA assay (ThermoFisher) or by low pass sequencing with a MiSeq nano kit (Illumina). Paired-end

100 cycle sequencing was performed on a NovaSeq 6000 (Illumina). RNAseq reads were aligned to the GRCm38 reference using STAR v2.7.1a[54] with Gencode MM10 annotations (vM25), and gene counts were assigned using featureCounts[55] from the Subread package (v1.5.1). For downstream analyses, predicted genes, processed pseudogenes, and genes with fewer than 5 counts relative to the mean library size (0.087 counts per million reads) were excluded from consideration. edgeR was used for CPM calculation and normalization,[56] limma was used to model differential expression between *Ripk1*$^{WT/REKA}$ *Mlkl*$^{-/-}$ and *Ripk1*$^{REKA/REKA}$ *Mlkl*$^{-/-}$ mice,[57] and Glimma was used for data exploration and visualization.[58] Gene Set Enrichment Analysis (GSEA)[59] was conducted for Hallmarks gene sets using GSEAPreranked with a classic scoring scheme and collapsing genes using the Mouse_Gene_Symbol_Remapping_MSigDB.v7.0.chip, and the ranked input was calculated by multiplying the limma-calculated log-fold changes by the inverse of the calculated p-values. RNAseq data were deposited into the Short Reach Archive (SRA) under BioProject accession PRJNA983782.

Flow cytometry and LPR quantification—Mouse spleens from indicated genotypes were mechanically digested, filtered (0.4μm), and RBC lysed for 3 min using RBC lysis buffer (154.4 mM NH_4Cl, 14.2 mM $NaHCO_3$, 1 mM EDTA, pH 7.3). After incubating 10% of the splenocytes (proportionally smaller % used for larger spleens) with Live/Dead Blue stain (Thermo Fisher Scientific), and anti-CD16/32 (Bio X Cell) to block FC receptors for 10 min at room temperature in the dark, they were stained with anti-CD45 (BD Biosciences), CD19 (BD Biosciences), B220 (Thermo Fisher Scientific), TCRβ (BD Biosciences), CD4 (BD Biosciences), and CD8 (BD Biosciences) for 30 min at room temperature in the dark. Compensation beads were used as single-color controls, then the stained cells were run on the 5-laser Aurora Spectral Flow Cytometer. Debris and dead cells (Live/Dead Blue positive) were excluded from analysis using FlowJo software before the described parameters were measured.

Histological, hematological and pathological analyses—Necropsy was performed by the St. Jude Comparative Pathology Core facility at the Animal Resources Center (St. Jude Children's Research Hospital). For histological examination, tissues were fixed in 10% (v/v) formalin in phosphate buffered saline (PBS), and sections were prepared and stained with H&E according to standard techniques. Tissue pathology was graded as follows: minimal 1+, mild 2+, moderate 3+, marked 4+. For differential cell counts, blood was collected into tubes containing EDTA (BD Microtainer, BD Diagnostics, Franklin Lakes, NJ) and peripheral blood counts were performed using a ForCyte Hematology Analyzer (Oxford Science, Inc, Oxford, CT) following the manufacturer's instructions.

Quantification and statistical analysis

Results in figures are graphically represented as mean ± SD. Statistics were perfroemd in GraphPad Prism. Statistical significance analysis was determined by using an unpaired *Student's t*-test and a two-way ANOVA analysis including a Tukey's multiple comparison test.

Supplementary Material

Refer to Web version on PubMed Central for supplementary material.

ACKNOWLEDGMENTS

This work was supported by National Institutes of Health AI44828 and CA231620 (to D.R.G.). B.T. is supported by King's College London.

REFERENCES

1. Tummers B, and Green DR (2022). The evolution of regulated cell death pathways in animals and their evasion by pathogens. Physiol. Rev. 102, 411–454. 10.1152/physrev.00002.2021. [PubMed: 34898294]
2. Alvarez-Diaz S, Dillon CP, Lalaoui N, Tanzer MC, Rodriguez DA, Lin A, Lebois M, Hakem R, Josefsson EC, O'Reilly LA, et al. (2016). The Pseudokinase MLKL and the Kinase RIPK3 Have Distinct Roles in Autoimmune Disease Caused by Loss of Death-Receptor-Induced Apoptosis. Immunity 45, 513–526. 10.1016/j.immuni.2016.07.016. [PubMed: 27523270]
3. Kaiser WJ, Upton JW, Long AB, Livingston-Rosanoff D, Daley-Bauer LP, Hakem R, Caspary T, and Mocarski ES (2011). RIP3 mediates the embryonic lethality of caspase-8-deficient mice. Nature 471, 368–372. 10.1038/nature09857. [PubMed: 21368762]
4. Oberst A, Dillon CP, Weinlich R, McCormick LL, Fitzgerald P, Pop C, Hakem R, Salvesen GS, and Green DR (2011). Catalytic activity of the caspase-8-FLIP(L) complex inhibits RIPK3-dependent necrosis. Nature 471, 363–367. 10.1038/nature09852. [PubMed: 21368763]
5. Tummers B, and Green DR (2022). Mechanisms of TNF-independent RIPK3-mediated cell death. Biochem. J. 479, 2049–2062. 10.1042/BCJ20210724. [PubMed: 36240069]
6. Cho YS, Challa S, Moquin D, Genga R, Ray TD, Guildford M, and Chan FKM (2009). Phosphorylation-driven assembly of the RIP1-RIP3 complex regulates programmed necrosis and virus-induced inflammation. Cell 137, 1112–1123. 10.1016/j.cell.2009.05.037. [PubMed: 19524513]
7. Holler N, Zaru R, Micheau O, Thome M, Attinger A, Valitutti S, Bodmer JL, Schneider P, Seed B, and Tschopp J (2000). Fas triggers an alternative, caspase-8-independent cell death pathway using the kinase RIP as effector molecule. Nat. Immunol. 1, 489–495. 10.1038/82732. [PubMed: 11101870]
8. Kaiser WJ, Sridharan H, Huang C, Mandal P, Upton JW, Gough PJ, Sehon CA, Marquis RW, Bertin J, and Mocarski ES (2013). Toll-like receptor 3-mediated necrosis via TRIF, RIP3, and MLKL. J. Biol. Chem. 288, 31268–31279. 10.1074/jbc.M113.462341. [PubMed: 24019532]
9. Ingram JP, Thapa RJ, Fisher A, Tummers B, Zhang T, Yin C, Rodriguez DA, Guo H, Lane R, Williams R, et al. (2019). ZBP1/DAI Drives RIPK3-Mediated Cell Death Induced by IFNs in the Absence of RIPK1. J. Immunol. 203, 1348–1355. 10.4049/jimmunol.1900216. [PubMed: 31358656]
10. Zhang T, Yin C, Boyd DF, Quarato G, Ingram JP, Shubina M, Ragan KB, Ishizuka T, Crawford JC, Tummers B, et al. (2020). Influenza Virus Z-RNAs Induce ZBP1-Mediated Necroptosis. Cell 180, 1115–1129.e13. 10.1016/j.cell.2020.02.050. [PubMed: 32200799]
11. Newton K, Dugger DL, Wickliffe KE, Kapoor N, de Almagro MC, Vucic D, Komuves L, Ferrando RE, French DM, Webster J, et al. (2014). Activity of protein kinase RIPK3 determines whether cells die by necroptosis or apoptosis. Science 343, 1357–1360. 10.1126/science.1249361. [PubMed: 24557836]
12. Dillon CP, Oberst A, Weinlich R, Janke LJ, Kang TB, Ben-Moshe T, Mak TW, Wallach D, and Green DR (2012). Survival function of the FADD-CASPASE-8-cFLIP(L) complex. Cell Rep. 1, 401–407. 10.1016/j.celrep.2012.03.010. [PubMed: 22675671]
13. Fritsch M, Günther SD, Schwarzer R, Albert MC, Schorn F, Werthenbach JP, Schiffmann LM, Stair N, Stocks H, Seeger JM, et al. (2019). Caspase-8 is the molecular switch

for apoptosis, necroptosis and pyroptosis. Nature 575, 683–687. 10.1038/s41586-019-1770-6. [PubMed: 31748744]

14. Newton K, Wickliffe KE, Maltzman A, Dugger DL, Reja R, Zhang Y, Roose-Girma M, Modrusan Z, Sagolla MS, Webster JD, and Dixit VM (2019). Activity of caspase-8 determines plasticity between cell death pathways. Nature 575, 679–682. 10.1038/s41586-019-1752-8. [PubMed: 31723262]
15. Mariathasan S, Newton K, Monack DM, Vucic D, French DM, Lee WP, Roose-Girma M, Erickson S, and Dixit VM (2004). Differential activation of the inflammasome by caspase-1 adaptors ASC and Ipaf. Nature 430, 213–218. 10.1038/nature02664. [PubMed: 15190255]
16. Kelliher MA, Grimm S, Ishida Y, Kuo F, Stanger BZ, and Leder P (1998). The death domain kinase RIP mediates the TNF-induced NF-kappaB signal. Immunity 8, 297–303. 10.1016/s1074-7613(00)80535-x. [PubMed: 9529147]
17. Dillon CP, Weinlich R, Rodriguez DA, Cripps JG, Quarato G, Gurung P, Verbist KC, Brewer TL, Llambi F, Gong YN, et al. (2014). RIPK1 blocks early postnatal lethality mediated by caspase-8 and RIPK3. Cell 157, 1189–1202. 10.1016/j.cell.2014.04.018. [PubMed: 24813850]
18. Rickard JA, O'Donnell JA, Evans JM, Lalaoui N, Poh AR, Rogers T, Vince JE, Lawlor KE, Ninnis RL, Anderton H, et al. (2014). RIPK1 regulates RIPK3-MLKL-driven systemic inflammation and emergency hematopoiesis. Cell 157, 1175–1188. 10.1016/j.cell.2014.04.019. [PubMed: 24813849]
19. Jang TH, Zheng C, Li J, Richards C, Hsiao YS, Walz T, Wu H, and Park HH (2014). Structural study of the RIPoptosome core reveals a helical assembly for kinase recruitment. Biochemistry 53, 5424–5431. 10.1021/bi500585u. [PubMed: 25119434]
20. Shutinoski B, Alturki NA, Rijal D, Bertin J, Gough PJ, Schloss-macher MG, and Sad S (2016). K45A mutation of RIPK1 results in poor necroptosis and cytokine signaling in macrophages, which impacts inflammatory responses in vivo. Cell Death Differ. 23, 1628–1637. 10.1038/cdd.2016.51. [PubMed: 27258786]
21. Yeh WC, de la Pompa JL, McCurrach ME, Shu HB, Elia AJ, Shahinian A, Ng M, Wakeham A, Khoo W, Mitchell K, et al. (1998). FADD: essential for embryo development and signaling from some, but not all, inducers of apoptosis. Science 279, 1954–1958. 10.1126/science.279.5358.1954. [PubMed: 9506948]
22. Varfolomeev EE, Schuchmann M, Luria V, Chiannilkulchai N, Beckmann JS, Mett IL, Rebrikov D, Brodianski VM, Kemper OC, Kollet O, et al. (1998). Targeted disruption of the mouse Caspase 8 gene ablates cell death induction by the TNF receptors, Fas/Apo1, and DR3 and is lethal prenatally. Immunity 9, 267–276. 10.1016/s1074-7613(00)80609-3. [PubMed: 9729047]
23. Yeh WC, Itie A, Elia AJ, Ng M, Shu HB, Wakeham A, Mirtsos C, Suzuki N, Bonnard M, Goeddel DV, and Mak TW (2000). Requirement for Casper (c-FLIP) in regulation of death receptor-induced apoptosis and embryonic development. Immunity 12, 633–642. 10.1016/s1074-7613(00)80214-9. [PubMed: 10894163]
24. Mrkvova Z, Portesova M, and Slaninova I (2021). Loss of FADD and Caspases Affects the Response of T-Cell Leukemia Jurkat Cells to Anti-Cancer Drugs. Int. J. Mol. Sci. 22, 2702. 10.3390/ijms22052702. [PubMed: 33800107]
25. Petersen SL, Wang L, Yalcin-Chin A, Li L, Peyton M, Minna J, Harran P, and Wang X (2007). Autocrine TNFalpha signaling renders human cancer cells susceptible to Smac-mimetic-induced apoptosis. Cancer Cell 12, 445–456. 10.1016/j.ccr.2007.08.029. [PubMed: 17996648]
26. He S, Liang Y, Shao F, and Wang X (2011). Toll-like receptors activate programmed necrosis in macrophages through a receptor-interacting kinase-3-mediated pathway. Proc. Natl. Acad. Sci. USA 108, 20054–20059. 10.1073/pnas.1116302108. [PubMed: 22123964]
27. Kim SJ, and Li J (2013). Caspase blockade induces RIP3-mediated programmed necrosis in Toll-like receptor-activated microglia. Cell Death Dis. 4, e716. 10.1038/cddis.2013.238. [PubMed: 23846218]
28. Mandal P, Berger SB, Pillay S, Moriwaki K, Huang C, Guo H, Lich JD, Finger J, Kasparcova V, Votta B, et al. (2014). RIP3 induces apoptosis independent of pronecrotic kinase activity. Mol. Cell 56, 481–495. 10.1016/j.molcel.2014.10.021. [PubMed: 25459880]

29. Nemazee DA, Studer S, Steinmetz M, Dembić Z, and Kiefer M (1985). The lymphoproliferating cells of MRL-lpr/lpr mice are a polyclonal population that bear the T lymphocyte receptor for antigen. Eur. J. Immunol. 15, 760–764. 10.1002/eji.1830150804. [PubMed: 4029256]
30. He S, Wang L, Miao L, Wang T, Du F, Zhao L, and Wang X (2009). Receptor interacting protein kinase-3 determines cellular necrotic response to TNF-alpha. Cell 137, 1100–1111. 10.1016/j.cell.2009.05.021. [PubMed: 19524512]
31. Zhang DW, Shao J, Lin J, Zhang N, Lu BJ, Lin SC, Dong MQ, and Han J (2009). RIP3, an energy metabolism regulator that switches TNF-induced cell death from apoptosis to necrosis. Science 325, 332–336. 10.1126/science.1172308. [PubMed: 19498109]
32. Upton JW, Kaiser WJ, and Mocarski ES (2012). DAI/ZBP1/DLM-1 complexes with RIP3 to mediate virus-induced programmed necrosis that is targeted by murine cytomegalovirus vIRA. Cell Host Microbe 11, 290–297. 10.1016/j.chom.2012.01.016. [PubMed: 22423968]
33. Kohchi C, Noguchi K, Tanabe Y, Mizuno D, and Soma G (1994). Constitutive expression of TNF-alpha and -beta genes in mouse embryo: roles of cytokines as regulator and effector on development. Int. J. Biochem. 26, 111–119. 10.1016/0020-711x(94)90203-8. [PubMed: 8138038]
34. Takaoka A, Wang Z, Choi MK, Yanai H, Negishi H, Ban T, Lu Y, Miyagishi M, Kodama T, Honda K, et al. (2007). DAI (DLM-1/ZBP1) is a cytosolic DNA sensor and an activator of innate immune response. Nature 448, 501–505. 10.1038/nature06013. [PubMed: 17618271]
35. Rodriguez DA, Quarato G, Liedmann S, Tummers B, Zhang T, Guy C, Crawford JC, Palacios G, Pelletier S, Kalkavan H, et al. (2022). Caspase-8 and FADD prevent spontaneous ZBP1 expression and necroptosis. Proc. Natl. Acad. Sci. USA 119, e2207240119. 10.1073/pnas.2207240119. [PubMed: 36191211]
36. Hartwig T, Montinaro A, von Karstedt S, Sevko A, Surinova S, Chakravarthy A, Taraborrelli L, Draber P, Lafont E, Arce Vargas F, et al. (2017). The TRAIL-Induced Cancer Secretome Promotes a Tumor-Supportive Immune Microenvironment via CCR2. Mol. Cell 65, 730–742.e5. 10.1016/j.molcel.2017.01.021. [PubMed: 28212753]
37. Henry CM, and Martin SJ (2017). Caspase-8 Acts in a Non-enzymatic Role as a Scaffold for Assembly of a Pro-inflammatory "FADDosome" Complex upon TRAIL Stimulation. Mol. Cell 65, 715–729.e5. 10.1016/j.molcel.2017.01.022. [PubMed: 28212752]
38. Schwarzer R, Jiao H, Wachsmuth L, Tresch A, and Pasparakis M (2020). FADD and Caspase-8 Regulate Gut Homeostasis and Inflammation by Controlling MLKL- and GSDMD-Mediated Death of Intestinal Epithelial Cells. Immunity 52, 978–993.e6. 10.1016/j.immuni.2020.04.002. [PubMed: 32362323]
39. Tummers B, Mari L, Guy CS, Heckmann BL, Rodriguez DA, Rühl S, Moretti J, Crawford JC, Fitzgerald P, Kanneganti TD, et al. (2020). Caspase-8-Dependent Inflammatory Responses Are Controlled by Its Adaptor, FADD, and Necroptosis. Immunity 52, 994–1006.e8. 10.1016/j.immuni.2020.04.010. [PubMed: 32428502]
40. Lalaoui N, Boyden SE, Oda H, Wood GM, Stone DL, Chau D, Liu L, Stoffels M, Kratina T, Lawlor KE, et al. (2020). Mutations that prevent caspase cleavage of RIPK1 cause autoinflammatory disease. Nature 577, 103–108. 10.1038/s41586-019-1828-5. [PubMed: 31827281]
41. Newton K, Wickliffe KE, Dugger DL, Maltzman A, Roose-Girma M, Dohse M, Kőműves L, Webster JD, and Dixit VM (2019). Cleavage of RIPK1 by caspase-8 is crucial for limiting apoptosis and necroptosis. Nature 574, 428–431. 10.1038/s41586-019-1548-x. [PubMed: 31511692]
42. Zhang Y, Huang K, Zhang Y, Han T, Li L, Ruan C, Sun YH, Shi W, Han W, Wu SQ, et al. (2021). A unique death pathway keeps RIPK1 D325A mutant mice in check at embryonic day 10.5. PLoS Biol. 19, e3001304. 10.1371/journal.pbio.3001304. [PubMed: 34437534]
43. Liu Y, Fan C, Zhang Y, Yu X, Wu X, Zhang X, Zhao Q, Zhang H, Xie Q, Li M, et al. (2017). RIP1 kinase activity-dependent roles in embryonic development of Fadd-deficient mice. Cell Death Differ. 24, 1459–1469. 10.1038/cdd.2017.78. [PubMed: 28574501]
44. Stocking C, and Kozak CA (2008). Murine endogenous retroviruses. Cell. Mol. Life Sci. 65, 3383–3398. 10.1007/s00018-008-8497-0. [PubMed: 18818872]

45. Jiao H, Wachsmuth L, Kumari S, Schwarzer R, Lin J, Eren RO, Fisher A, Lane R, Young GR, Kassiotis G, et al. (2020). Z-nucleic-acid sensing triggers ZBP1-dependent necroptosis and inflammation. Nature 580, 391–395. 10.1038/s41586-020-2129-8. [PubMed: 32296175]
46. Lin J, Kumari S, Kim C, Van TM, Wachsmuth L, Polykratis A, and Pasparakis M (2016). RIPK1 counteracts ZBP1-mediated necroptosis to inhibit inflammation. Nature 540, 124–128. 10.1038/nature20558. [PubMed: 27819681]
47. Newton K, Wickliffe KE, Maltzman A, Dugger DL, Strasser A, Pham VC, Lill JR, Roose-Girma M, Warming S, Solon M, et al. (2016). RIPK1 inhibits ZBP1-driven necroptosis during development. Nature 540, 129–133. 10.1038/nature20559. [PubMed: 27819682]
48. Meng H, Liu Z, Li X, Wang H, Jin T, Wu G, Shan B, Christofferson DE, Qi C, Yu Q, et al. (2018). Death-domain dimerization-mediated activation of RIPK1 controls necroptosis and RIPK1-dependent apoptosis. Proc. Natl. Acad. Sci. USA 115, E2001–E2009. 10.1073/pnas.1722013115. [PubMed: 29440439]
49. Anderton H, Bandala-Sanchez E, Simpson DS, Rickard JA, Ng AP, Di Rago L, Hall C, Vince JE, Silke J, Liccardi G, and Feltham R (2019). RIPK1 prevents TRADD-driven, but TNFR1 independent, apoptosis during development. Cell Death Differ. 26, 877–889. 10.1038/s41418-018-0166-8. [PubMed: 30185824]
50. Newton K, Sun X, and Dixit VM (2004). Kinase RIP3 is dispensable for normal NF-kappa Bs, signaling by the B-cell and T-cell receptors, tumor necrosis factor receptor 1, and Toll-like receptors 2 and 4. Mol. Cell Biol. 24, 1464–1469. 10.1128/MCB.24.4.1464-1469.2004. [PubMed: 14749364]
51. Murphy JM, Czabotar PE, Hildebrand JM, Lucet IS, Zhang JG, Alvarez-Diaz S, Lewis R, Lalaoui N, Metcalf D, Webb AI, et al. (2013). The pseudokinase MLKL mediates necroptosis via a molecular switch mechanism. Immunity 39, 443–453. 10.1016/j.immuni.2013.06.018. [PubMed: 24012422]
52. Pelletier S, Gingras S, and Green DR (2015). Mouse genome engineering via CRISPR-Cas9 for study of immune function. Immunity 42, 18–27. 10.1016/j.immuni.2015.01.004. [PubMed: 25607456]
53. Bae S, Park J, and Kim JS (2014). Cas-OFFinder: a fast and versatile algorithm that searches for potential off-target sites of Cas9 RNA-guided endonucleases. Bioinformatics 30, 1473–1475. 10.1093/bioinformatics/btu048. [PubMed: 24463181]
54. Dobin A, Davis CA, Schlesinger F, Drenkow J, Zaleski C, Jha S, Batut P, Chaisson M, and Gingeras TR (2013). STAR: ultrafast universal RNA-seq aligner. Bioinformatics 29, 15–21. 10.1093/bioinformatics/bts635. [PubMed: 23104886]
55. Liao Y, Smyth GK, and Shi W (2014). featureCounts: an efficient general purpose program for assigning sequence reads to genomic features. Bioinformatics 30, 923–930. 10.1093/bioinformatics/btt656. [PubMed: 24227677]
56. Robinson MD, McCarthy DJ, and Smyth GK (2010). edgeR: a Bioconductor package for differential expression analysis of digital gene expression data. Bioinformatics 26, 139–140. 10.1093/bioinformatics/btp616. [PubMed: 19910308]
57. Ritchie ME, Phipson B, Wu D, Hu Y, Law CW, Shi W, and Smyth GK (2015). limma powers differential expression analyses for RNA-sequencing and microarray studies. Nucleic Acids Res. 43, e47. 10.1093/nar/gkv007. [PubMed: 25605792]
58. Su S, Law CW, Ah-Cann C, Asselin-Labat ML, Blewitt ME, and Ritchie ME (2017). Glimma: interactive graphics for gene expression analysis. Bioinformatics 33, 2050–2052. 10.1093/bioinformatics/btx094. [PubMed: 28203714]
59. Subramanian A, Tamayo P, Mootha VK, Mukherjee S, Ebert BL, Gillette MA, Paulovich A, Pomeroy SL, Golub TR, Lander ES, and Mesirov JP (2005). Gene set enrichment analysis: a knowledge-based approach for interpreting genome-wide expression profiles. Proc. Natl. Acad. Sci. USA 102, 15545–15550. 10.1073/pnas.0506580102. [PubMed: 16199517]

Highlights

- A mutation in RIPK1 (R588E) disrupts the interaction between RIPK1 and FADD
- Disrupting the interaction between RIPK1 and FADD leads to embryonic lethality
- The kinase activity of RIPK1 R588E prevents RIPK3-mediated embryonic lethality
- *Zbp1* ablation partially prevents RIPK1 R588E-mediated embryonic lethality

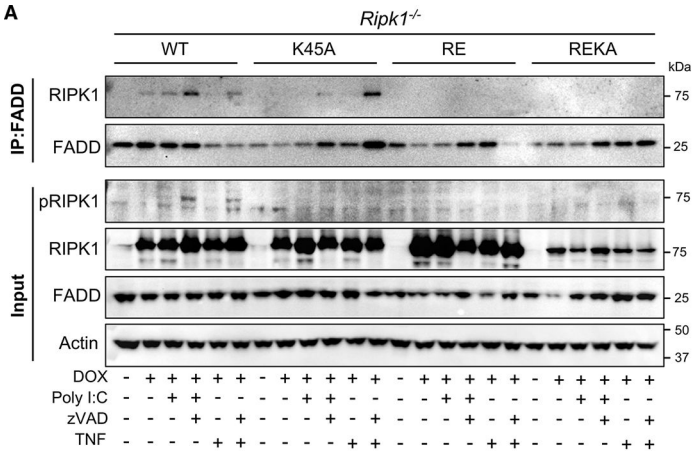

B

$Ripk1^{RE/WT}$ x $Ripk1^{RE/WT}$

Genotype \ Embryonic stage	E10.5 - E13.5	E14.5 - E16.5	E16.5 - E19.5	Born
$Ripk1^{WT/WT}$	13 / (11.25)	8 / (7)	7 / (4.75)	76 / (60.25)
$Ripk1^{RE/WT}$	27 / (22.5)	15 / (14)	12 / (9.5)	165 / (120.5)
$Ripk1^{RE/RE}$	5 / (11.25)	5 / (7)	0 / (4.75)	0 / (60.25)
Total	45	28	19	241

Observed / Expected values (%)

C

$Ripk1^{REKA/WT}$ x $Ripk1^{REKA/WT}$

Genotype \ Embryonic stage	E10.5 - E13.5	E14.5 - E16.5	E16.5 - E19.5	Born
$Ripk1^{WT/WT}$	9 / (6.25)	4 / (6.25)	12 / (9.5)	46 / (29.25)
$Ripk1^{REKA/WT}$	7 / (12.5)	16 / (12.5)	22 / (19)	71 / (58.5)
$Ripk1^{REKA/REKA}$	9 / (6.25)	5 / (6.25)	4 / (9.5)	0 / (29.25)
Total	25	25	38	117

Observed / Expected values (%)

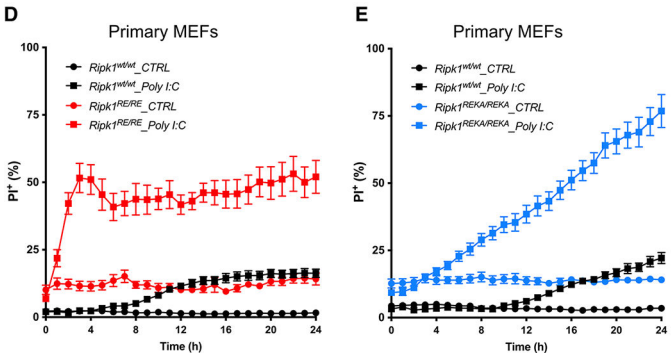

Figure 1. The point mutation R588E at RIPK1 DD disrupts RIPK1-FADD interaction and confers embryonic lethality

(A) Immunoprecipitation of FADD in *Ripk1*$^{-/-}$ MEFs reconstituted with doxycycline (DOX)-inducible RIPK1 (WT), RIPK1-K45A (K45A), RIPK1-R588E (RE), or RIPK1-K45A/R588E (REKA) and incubated 2 h with DOX (1 mg/mL) in the absence or presence of poly I:C (100 μg/mL) or TNF (10 ng/mL) plus zVAD (50 μM). Immunoprecipitates were collected and RIPK1-FADD interaction assessed by immunoblotting using the indicated antibodies.

Representative of 2 independent experiments.

(B) Observed numbers of offspring of *Ripk1*$^{RE/WT}$ intercrosses at E10.5–E13.5, E14.5–E16.5, and E16.5–E19.5 post-gestation.
(C) Observed numbers of offspring of *Ripk1*$^{REKA/WT}$ intercrosses at E10.5–E13.5, E14.5–E16.5, and E16.5–E19.5 post-gestation.
(D and E) Quantification of cell death in primary MEFs expressing endogenous *Ripk1*$^{RE/RE}$ (D) or *Ripk1*$^{REKA/REKA}$ (E) versus their respective littermate-derived *Ripk1*$^{WT/WT}$ controls. Cells were treated with 100 μg/mL poly I:C, and the kinetics of cell death were monitored by propidium iodide (PI^+ %) uptake using an Incucyte Kinetic Live Cell Imager. Representative of three independent experiments. Data are presented as mean ± SD.
See also Figures S1 and S2.

A

Ripk1$^{RE/WT}$ *Ripk3*$^{-/-}$ x *Ripk1*$^{RE/WT}$ *Ripk3*$^{-/-}$

	Ripk3$^{-/-}$ (n=66)		
Ripk1	*WT/WT*	*RE/WT*	*RE/RE*
Expected	16.5	33	16.5
Observed	20	28	18

B

Ripk1$^{REKA/WT}$ *Ripk3*$^{-/-}$ x *Ripk1*$^{REKA/WT}$ *Ripk3*$^{-/-}$

	Ripk3$^{-/-}$ (n=63)		
Ripk1	*WT/WT*	*REKA/WT*	*REKA/REKA*
Expected	15.75	31.5	15.75
Observed	12	37	14

C

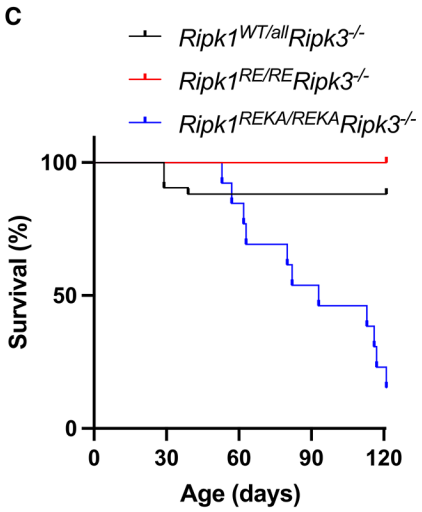

Figure 2. RIPK3 drives death of developing *Ripk1*$^{RE/RE}$ and *Ripk1*$^{REKA/REKA}$ embryos

(A and B) Expected Mendelian ratios and observed numbers of offspring of *Ripk1*$^{RE/WT}$ *Ripk3*$^{-/-}$ intercrosses (n = 66) (A) or *Ripk1*$^{REKA/WT}$ *Ripk3*$^{-/-}$ intercrosses (n = 63) (B). (C) Post-natal survival up to 120 days of *Ripk1*$^{WT/all}$ *Ripk3*$^{-/-}$ (n = 42), *Ripk1*$^{RE/RE}$ *Ripk3*$^{-/-}$ (n = 8), and *Ripk1*$^{REKA/REKA}$ *Ripk3*$^{-/-}$ (n = 13) animals. WT/all indicates that both heterozygotes and WT/WT genotypes were analyzed together.

A

Ripk1$^{RE/WT}$ *Mlkl*$^{-/-}$ x *Ripk1*$^{RE/WT}$ *Mlkl*$^{-/-}$

	Mlkl$^{-/-}$ (n=400)		
Ripk1	*WT/WT*	*RE/WT*	*RE/RE*
Expected	100	200	100
Observed	118	229	53

B

Mlkl$^{-/-}$

Ripk1	*WT/WT*	*RE/WT*	*RE/RE*
Born	39	79	18
Weaned	37	77	7

C

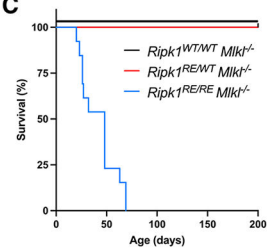

D Colon

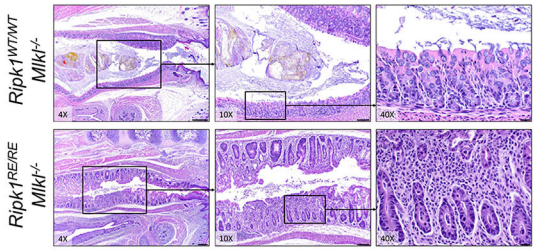

E Skin

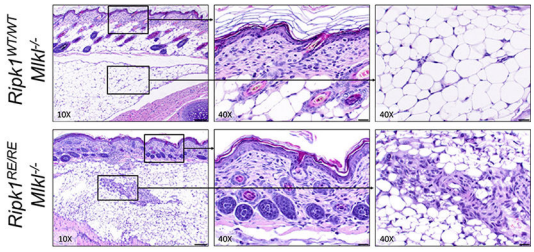

F

Ripk1$^{RE/WT}$ *Mlkl*$^{-/-}$ vs *Ripk1*$^{RE/RE}$ *Mlkl*$^{-/-}$

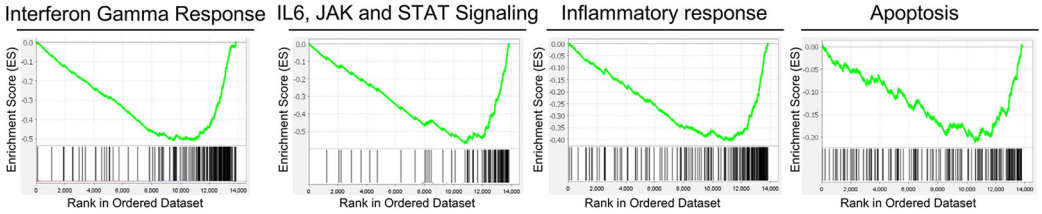

G

Ripk1$^{RE/WT}$ *Fadd*$^{+/-}$ *Mlkl*$^{-/-}$ x *Ripk1*$^{RE/WT}$ *Fadd*$^{+/-}$ *Mlkl*$^{-/-}$

	Fadd$^{+/+}$ (n=51)		
Ripk1	*WT/WT*	*RE/WT*	*RE/RE*
Expected	12.75	25.5	12.75
Observed	15	28	8
	Fadd$^{+/-}$ (n=101)		
Ripk1	*WT/WT*	*RE/WT*	*RE/RE*
Expected	25.25	50.5	25.25
Observed	29	55	17
	Fadd$^{-/-}$ (n=44)		
Ripk1	*WT/WT*	*RE/WT*	*RE/RE*
Expected	11	22	11
Observed	9	16	18

Total = 196

H

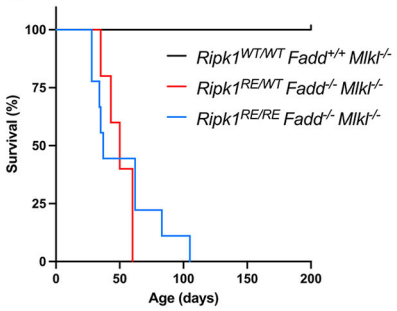

Figure 3. The RIPK1-FADD interaction negatively controls RIPK3-mediated lethal inflammation

(A) Expected Mendelian ratios and observed numbers of offspring of *Ripk1*$^{RE/WT}$ *Mlkl*$^{-/-}$ intercrosses (n = 400).

(B) Observed numbers of offspring of *Ripk1*$^{RE/WT}$ *Mlkl*$^{-/-}$ intercrosses at birth (present at post-natal day 3 [P3]) and at weaning (P21).

(C) Post-natal survival up to 200 days of *Ripk1*$^{WT/WT}$ *Mlkl*$^{-/-}$ (n = 13), *Ripk1*$^{RE/WT}$ *Mlkl*$^{-/-}$ (n = 13), and *Ripk1*$^{RE/RE}$ *Mlkl*$^{-/-}$ (n = 13) animals.

(D and E) H&E staining of colon (D) or skin (E) tissue of *Ripk1*$^{WT/WT}$ *Mlkl*$^{+/+}$ (top) and *Ripk1*$^{RE/RE}$ *Mlkl*$^{-/-}$ (bottom) mice. Magnified areas (4×, scale bar: 200 μm; 10×, scale bar: 100 μm; and 40×, scale bar: 20 μm, respectively) are indicated. Images represent 2 independent experiments.

(F) Selected Hallmarks pathway enrichment score plots of RNA sequencing gene set enrichment analysis comparing liver transcriptomes of *Ripk1*$^{RE/WT}$ *Mlkl*$^{-/-}$ and *Ripk1*$^{RE/RE}$ *Mlkl*$^{-/-}$ mice. Calculation and analysis are described in the STAR Methods.

(G) Expected Mendelian ratios and observed numbers of offspring of *Ripk1*$^{RE/WT}$ *Fadd*$^{-/+}$ *Mlkl*$^{-/-}$ intercrosses (n = 196).

(H) Post-natal survival up to 200 days of *Ripk1*$^{WT/WT}$ *Fadd*$^{+/+}$ *Mlkl*$^{-/-}$ (n = 5), *Ripk1*$^{RE/WT}$ *Fadd*$^{-/-}$ *Mlkl*$^{-/-}$ (n = 5), and *Ripk1*$^{RE/RE}$ *Fadd*$^{-/-}$ *Mlkl*$^{-/-}$ (n = 9) animals.

See also Figure S3.

A

Ripk1$^{REKA/WT}$ *Mlkl*$^{-/-}$ x *Ripk1*$^{REKA/WT}$ *Mlkl*$^{-/-}$

	Mlkl$^{-/-}$ (n=63)		
Ripk1	*WT/WT*	*REKA/WT*	*REKA/REKA*
Expected	51.25	102.5	51.25
Observed	77	128	0

B

Ripk1$^{REKA/WT}$ *Casp8*$^{+/-}$ *Mlkl*$^{-/-}$ x *Ripk1*$^{REKA/WT}$ *Casp8*$^{+/-}$ *Mlkl*$^{-/-}$

	Casp8$^{+/+}$ (n=57)		
Ripk1	*WT/WT*	*REKA/WT*	*RE/RE*
Expected	14.25	28.5	14.25
Observed	25	32	0
	Casp8$^{+/-}$ (n=69)		
Ripk1	*WT/WT*	*REKA/WT*	*REKA/REKA*
Expected	17.5	34.5	17.5
Observed	26	43	0
	Casp8$^{-/-}$ (n=54)		
Ripk1	*WT/WT*	*REKA/WT*	*REKA/REKA*
Expected	13.25	27	13.25
Observed	20	23	11

Total = 180

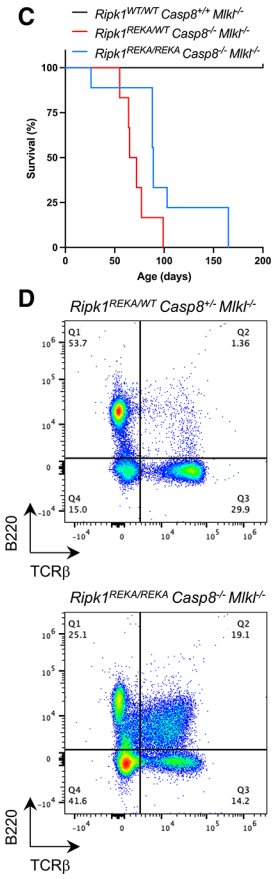

Figure 4. Ablation of *Casp8* prevents embryonic lethality of *Ripk1*$^{REKA/REKA}$ *Mlkl*$^{-/-}$ mice

(A) Expected Mendelian ratios and observed numbers of offspring of *Ripk1*$^{REKA/WT}$ *Mlkl*$^{-/-}$ intercrosses (n = 205).

(B) Expected Mendelian ratios and observed numbers of offspring of *Ripk1*$^{RE/WT}$ *Casp8*$^{+/-}$ *Mlkl*$^{-/-}$ intercrosses (n = 180).

(C) Post-natal survival up to 200 days of *Ripk1*$^{WT/WT}$ *Casp8*$^{+/+}$ *Mlkl*$^{-/-}$ (n = 7), *Ripk1*$^{REKA/WT}$ *Casp8*$^{-/-}$ *Mlkl*$^{-/-}$ (n = 6), and *Ripk1*$^{REKA/REKA}$ *Casp8*$^{-/-}$ *Mlkl*$^{-/-}$ (n = 9) animals.

(D) Dot plots showing the presence of TCRβ+ and/or B220+ cells in peripheral blood of one representative mouse per indicated genotype as determined by flow cytometry.

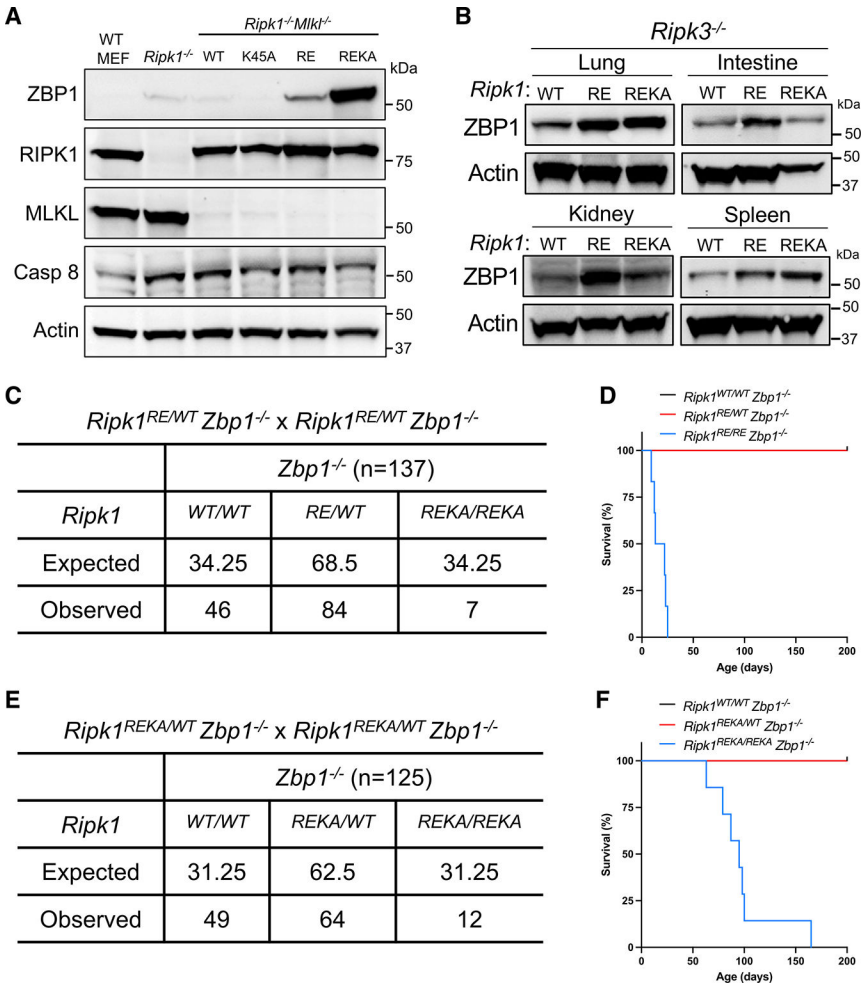

Figure 5. ZBP1 drives RIPK3-mediated death of *Ripk1*$^{RE/RE}$ and *Ripk1*$^{REKA/REKA}$ embryos

(A) WT, *Ripk1*$^{-/-}$, or *Ripk1*$^{-/-}$ *Mlkl*$^{-/-}$ MEFs reconstituted with RIPK1 (WT), RIPK1-K45A (K45A), RIPK1-R588E (RE), or RIPK1-R588E/K45A (REKA) were analyzed by immunoblotting using indicated antibodies. Representative of two independent experiments.

(B) Tissues from 4- to 6-week-old *Ripk1*$^{WT/WT}$ (WT), *Ripk1*$^{RE/RE}$ *Ripk3*$^{-/-}$ (RE), or *Ripk1*$^{REKA/REKA}$ *Ripk3*$^{-/-}$ (REKA) mice were examined by immunoblotting using indicated antibodies. Representative of two independent mice.

(C) Expected Mendelian ratios and observed numbers of offspring of *Ripk1*$^{RE/WT}$ *Zbp1*$^{-/-}$ intercrosses (n = 137).

(D) Expected Mendelian ratios and observed numbers of offspring from *Ripk1*$^{REKA/WT}$ *Zbp1*$^{-/-}$ intercrosses (n = 125).

(E) Post-natal survival up to 200 days of *Ripk1*$^{WT/WT}$ *Zbp1*$^{-/-}$ (n = 5), Ripk1RE/WT *Zbp1*$^{-/-}$ (n = 5), and *Ripk1*$^{RE/RE}$ *Zbp1*$^{-/-}$ (n = 5) mice.

(F) Post-natal survival up to 200 days of Ripk1$^{WT/WT}$ *Zbp1*$^{-/-}$ (n = 7), *Ripk1*$^{REKA/WT}$ *Zbp1*$^{-/-}$ (n = 7), and *Ripk1*$^{REKA/REKA}$ *Zbp1*$^{-/-}$ (n = 7) mice.

See also Figure S4.

KEY RESOURCES TABLE

REAGENT or RESOURCE	SOURCE	IDENTIFIER
Antibodies		
anti-β-Actin-HRP	Santa Cruz Technologies	Cat# sc-47778; RRID:AB_2714189
anti-Caspase 8	Cell signaling Technology	Cat# 4790; RRID:AB_10545768
anti-FADD	Abcam	Cat# ab124812; RRID:AB_10976310
anti-FADD	Santa Cruz Technologies	Cat# sc-271748; RRID:AB_10708849
anti-MLKL	Abgent	Cat# AP14272b; RRID:AB_11134649
anti-Phospho-RIP (Ser166)	Cell signaling Technology	Cat# 31122; RRID:AB_2799000
anti-RIPK1	Cell signaling Technology	Cat# 47783; RRID:AB_2799330
anti-RIPK1	Cell signaling Technology	Cat# 3493; RRID:AB_2305314
anti-RIPK3	Cell signaling Technology	Cat# 95702; RRID:AB_2721823
anti-ZBP1	AdipoGen 1	Cat# AG-20B-0010; RRID:AB_249019
LIVE/DEAD™ Fixable Blue Dead Cell Stain Kit, for UV excitation	Thermo Fisher Scientific	Cat# L34962
V500 Rat Anti-Mouse CD45	BD Biosciences	Cat# 561487
BUV395 Rat Anti-Mouse CD45	BD Biosciences	Cat# 564279
BUV615 Rat Anti-Mouse CD19	BD Biosciences	Cat# 751213
CD45R (B220) Monoclonal Antibody (RA3-6B2), APC780	Thermo Fisher Scientific	Cat# 47-0452-82
CD45R (B220) Monoclonal Antibody (RA3-6B2), PE-Cyanine7	Thermo Fisher Scientific	Cat# 25-0452-82
FITC Hamster Anti-Mouse TCR β Chain	BD Biosciences	Cat# 553170
BUV805 Rat Anti-Mouse CD8a	BD Biosciences	Cat# 612898
BUV737 Rat Anti-Mouse CD4	BD Biosciences	Cat# 564933
Anti-CD16/32 (FC Block)	Bio X Cell	Cat# BE0307
Chemicals, peptides, and recombinant proteins		
Amersham ECL Prime Western Blotting Detection Reagent	GE Lifesciences	Cat# RPN2232
Digitonin	Sigma-Aldrich	Cat# D141
DMEM	Thermo Fischer Scientific	Cat# 11995-073
Doxycycline (by Clontech)	Thermo Fischer Scientific	Cat# NC0424034
L-Glutamine	Thermo Fischer Scientific	Cat# 25030081
Nec1s	Calbiochem	Cat# 5.04297.0001
Non-essential amino acids	Thermo Fischer Scientific	Cat# 11140-050
Penicillin and streptomycin	Thermo Fischer Scientific	Cat# 15070-063
Phosphatase inhibitor cocktail	Roche	Cat# 04 906 837 001
Protease inhibitor cocktail	Roche	Cat# 04 693 159 001

REAGENT or RESOURCE	SOURCE	IDENTIFIER
Propidium Iodide Solution	Sigma-Aldrich	Cat# 537060
Poly I:C	Invivogen	Cat# tlrl-pic
Recombinant Murine TNF	Prepotech	Cat# 315-01A
Restriction enzyme AgeI	New England BioLabs	Cat# R3552L
Restriction enzyme HindIII	New England BioLabs	Cat# R0104L
RIPK3 inhibitor (GSK'872)	Invivogen	Cat# V2773
Sterile PBS	GIBCO	Cat# 14190-144
XT sample buffer 4x	Bio-Rad	Cat# 161-0791
zVAD-FMK	APExBIO	Cat# A1902
Critical commercial assays		
Dynabeads Co-Immunoprecipitation Kit	Invitrogen	Cat# 14321D
RNeasy Mini Kit	QIAGEN	Cat# 74104
Deposited data		
RNA sequencing data	This paper	SRA: PRJNA983782
Experimental models: Cell lines		
Immortalized *Ripk1*$^{-/-}$ MEFs	Dillon et al. [17]	N/A
Immortalized *Ripk1*$^{-/-}$ *Mlkl*$^{-/-}$ MEFs	Alvarez-Diaz et al. [2]	N/A
Primary *Ripk1*$^{R588E/R588E}$ MEFs	This paper	N/A
Primary *Ripk1*$^{R588E\text{-}K45A/R588E\text{-}K45A}$ MEFs	This paper	N/A
Experimental models: Organisms/strains		
Ripk1$^{R588E/R588E}$	This paper	N/A
Ripk1$^{R588E/R588E}$ *Mlkl*$^{-/-}$	This paper	N/A
Ripk1$^{R588E/R588E}$ *Ripk3*$^{-/-}$	This paper	N/A
Ripk1$^{R588E/R588E}$ *Zbp1*$^{-/-}$	This paper	N/A
Ripk1$^{R588E/R588E}$ *Fadd*$^{-/-}$ *Mlkl*$^{-/-}$	This paper	N/A
Ripk1$^{R588E\text{-}K45A/R588E\text{-}K45A}$	This paper	N/A
Ripk1 $^{R588E\text{-}K45A/R588E\text{-}K45A}$ *Mlkl*$^{-/-}$	This paper	N/A
Ripk1 $^{R588E\text{-}K45A/R588E\text{-}K45A}$ *Ripk3*$^{-/-}$	This paper	N/A
Ripk1 $^{R588E\text{-}K45A/R588E\text{-}K45A}$ *Zbp1*$^{-/-}$	This paper	N/A
Ripk1 $^{R588E\text{-}K45A/R588E\text{-}K45A}$ *Casp8*$^{-/-}$ *Mlkl*$^{-/-}$	This paper	N/A
Oligonucleotides		
R588E single-guide RNA (sgRNA): 5'-GAAAAACTGTGCCCGCAAGC-3	This paper	N/A
Ripk1-R588E-HDR (Homology Directed Repair): 5'-TGAACACCTGAACCCTATCAGGGAAAACC TGGGAAGGCAGTGGAAAAACTGTGCC**GAG** AAGCT**T**GGCTTCACTGAGTCTCAGATCGAT GAAATCGACCATGACTATGAAAGAGATGG	This paper	N/A

REAGENT or RESOURCE	SOURCE	IDENTIFIER
ACTGAAAG-3' (underscored is the HindIII site, bold mutated sites)		
R588E PCR: forward 5'- ACATCTGCCGAGGAGGAAAC -3'	This paper	N/A
R588E PCR: reverse 5'- CTACTGGTCATGGACCGACC -3'	This paper	N/A
K45A single-guide RNA (sgRNA): 5' -TCCTGAAAAAAGTATACACA-3	This paper	N/A
Ripk1-K45A-HDR (Homology Directed Repair): 5'-AGGCTTCGGGAAGGTGTCCTTGTGTTAC CACAGAAGCCATGGATTTGTCATCCTG**GCG** AAAGT**C**TACAC**C**GG**T**CCCAACCGCGCTGAG TGAGTTGGGGGCATAAATGGGCTTGGCTTT TTGCTAGCTGAC-3' (underscored is the AgeI site, bold mutated sites)	This paper	N/A
K45A PCR: forward 5'- CGGTCCTTTTGCCCTGAGAC-3'	This paper	N/A
K45A PCR: reverse 5'- AAAAAGGCGCCCCTCTCAA-3'	This paper	N/A
Recombinant DNA		
pBABE-puro plasmid	Addgene	Cat# 1764
pRetroX-TRE3G plasmid	Clontech	Cat# 631188
Software and algorithms		
GraphPad Prism 9.0	GraphPad	https://www.graphpad.com
Incucyte® Live-Cell Analysis System	Sartorius	https://www.sartorius.com
ChemiDoc Imaging System	Bio-Rad	https://www.bio-rad.com/en-us/category/chemidoc-imaging-systems?ID=NINJ0Z15